capstract:2611.00047v1 [physics.ao-ph] 20 Nov 2026

A Recharge-Oscillator Model of Overnight Duvet Displacement in Shared Beds, with Phase Locking to the Ultradian Sleep Cycle

Tomas R. Eklund-Okafor,[1,*] Priya N. Venkataraghavan,[1,2] and Daniel H. Marchetti-Lowe[2]

[1]*Department of Atmospheric and Oceanic Sciences, Fjellvik Institute of Technology, 9120 Fjellvik, Norway*
[2]*Sleep and Chronobiology Unit, Calderbeck Hospital Research Centre, Calderbeck CB4 2NT, United Kingdom*

(Dated: November 20, 2026)

Two people sharing one duvet rarely keep it where it started. We treat the lateral position of the duvet on a double bed as a single climate-like index, and ask whether its overnight evolution is better described by a two-variable recharge oscillator of the kind used for the El Niño–Southern Oscillation (ENSO) than by red noise or a delayed-action oscillator. The index is the centroid of the duvet footprint relative to the mattress centreline, measured at 1 Hz by a ceiling-mounted depth camera over 192 nights in 64 cohabiting couples. The companion variable is the net fabric draped over the two long edges, which plays the role of warm water volume. Pooled regression gives an oscillation period of 143 min (95% interval 136–152 min) and an amplitude damping time of 100 min. The ensemble spectrum exceeds a matched AR(1) null by a factor of 5.4 at 0.44 cycles per hour, and the companion variable leads the index by 36 min, a quarter period. Transfer events have a mean phase of 9° after the end of each REM episode (Rayleigh test, 61 of 64 couples individually significant at $p < 0.01$), and the lagged coherence of the index depends on the ultradian phase at which it is started, in the manner of the ENSO spring predictability barrier. At 30 to 120 min lead the recharge model outperforms persistence and lag regression, and at 180 min it does not.

PACS numbers: 92.10.am, 92.70.Gt, 87.19.rm

I. INTRODUCTION

A duvet on a double bed does not stay put. Sleepers turn over many times a night (Wilde-Frenz and Schulz, 1983), and each turn moves some fabric with it. The thermal consequences are not trivial: skin temperature and bedding microclimate both bear on sleep onset and sleep continuity (Raymann et al., 2005; Okamoto-Mizuno and Mizuno, 2012). Questionnaire studies of bed-sharing couples report that disagreement over the cover is common and that most pairs settle into a habitual pattern of who ends up with more of it (Sandoval and Ek, 2019). We have not found a dynamical description of how a single cover is partitioned between two sleepers over the course of a night, as opposed to a tally of how often it goes wrong.

The quantity is simple enough to be treated as a one-dimensional field. If $T(t)$ is the lateral position of the duvet relative to the centreline of the mattress, then a displacement toward one occupant uncovers the other, the uncovered occupant responds, and the response eventually carries the duvet back. This is the structure of the equatorial Pacific in Bjerknes's picture of ENSO, where a warm anomaly in the east weakens the winds that sustain it, and the ocean adjusts over a time scale set by wave propagation and by the discharge of heat from the equatorial band (Bjerknes, 1969; Wyrtki, 1975). Three families of low-order models have been used for the oscillation that results. The delayed-action oscillator closes the loop with a negative feedback that arrives after a wave transit time δ (Suarez and Schopf, 1988; Battisti and Hirst, 1989). The recharge oscillator replaces the delay with a second state variable, the equatorial warm water volume h, which leads the sea surface temperature anomaly by roughly a quarter cycle (Jin, 1997; Burgers et al., 2005). The stochastic view dispenses with an oscillator altogether and treats the index as a damped linear mode driven by weather noise (Hasselmann, 1976; Penland and Sardeshmukh, 1995). Seasonal modulation of the growth rate or the noise adds phase locking of events to the calendar year and, in some formulations, a staircase of locked periods (Jin et al., 1994; Tziperman et al., 1994), while the dependence of persistence on the starting month is the spring predictability barrier (Webster and Yang, 1992). The observed period, 2 to 7 years, is long relative to the annual forcing (McPhaden et al., 2006).

The bed has a second periodic process of its own. Sleep is organised into cycles of NREM and REM sleep with a length of about 90 min (Dement and Kleitman, 1957), and gross body movements cluster at the transitions between stages (Wilde-Frenz and Schulz, 1983). If duvet transfers are driven by body movements, then the ultradian cycle plays the part of the annual cycle.

This gives four testable statements. First, the spectrum of T should have a peak above that of a red-noise process with the same one-step autocorrelation, at the period predicted by the fitted oscillator. Second, h should lead T by a quarter period. Third, transfer events should be locked to the phase of the ultradian cycle, and the coherence of T across a given lag should depend on the phase at which the lag starts. Fourth, a

* teklund@aos.fjellvik-tech.no

forecast that carries h should outperform persistence and lag regression at leads near a quarter to a full period. We test these on 192 nights from 64 couples. The model is set out in Sec. II, the measurements in Sec. III, the results in Sec. IV, and limitations in Sec. V.

II. MODEL

A. State variables

The duvet displacement index (DDI), T, is the lateral coordinate of the centroid of the duvet footprint measured from the mattress centreline and divided by half the mattress width. It is positive toward occupant A, who is defined as the occupant on the left as seen from the camera. The overhang asymmetry h is the mass of duvet draped over the A-side long edge minus that over the B-side long edge, expressed in the same nominal units as T. Fabric that hangs over an edge stores weight that is released as a restoring force on the cover, so h accumulates while the duvet is displaced and discharges as it returns. Only the product of the coupling coefficients F and A below is identified by the data, because the scale of h is arbitrary. We therefore report them separately only for a fixed scaling of h, given in Sec. III.B.

B. Recharge oscillator

We write the model in the form used by Burgers et al. (2005),

$$\frac{dT}{dt} = R\,T + F\,h + \sigma(t)\,\xi(t), \qquad \frac{dh}{dt} = -A\,T - r\,h, \tag{1}$$

where ξ is white noise with unit spectral density and $\sigma(t)$ the noise amplitude. The coefficient R is the net growth rate of the displacement, the difference between a positive feedback (an uncovered sleeper pulls harder) and local damping, r is the discharge rate of the overhang, and F and A couple the two variables. The deterministic part has eigenvalues $-\gamma \pm i\omega$ with

$$\gamma = \frac{r - R}{2}, \qquad \omega^2 = F A - \left(\frac{R + r}{2}\right)^2, \qquad P = \frac{2\pi}{\omega}. \tag{2}$$

The oscillation decays when $r > R$ and is sustained only by σ. In the stationary state h leads T by a quarter period when $\gamma \ll \omega$, and by somewhat less otherwise.

C. Delayed-action alternative

The delayed-action form is

$$\frac{dT}{dt} = R\,T(t) - \kappa\,T(t - \delta) + \sigma(t)\,\xi(t), \tag{3}$$

in which the period of the resulting oscillation lies between 2δ and 4δ (Suarez and Schopf, 1988). We fit κ and δ to T alone and check the fitted δ against the spectral peak. A pure red-noise null is an AR(1) process with the same variance and one-step autocorrelation as the data (Penland and Sardeshmukh, 1995).

D. Ultradian modulation

We allow the noise amplitude to vary with the phase of the sleep cycle,

$$\sigma(t) = \sigma_0 \left[1 + \epsilon \cos\!\left(\frac{2\pi t}{P_s} - \varphi\right)\right], \tag{4}$$

where P_s is the length of the current NREM–REM cycle. We define phase zero at the offset of a REM episode and, for the first cycle, at sleep onset. The modulation depth ϵ and phase φ are estimated from the residual variance of Eq. (1) as a function of phase. Because the noise and not the growth rate carries the modulation, the model has no parametric resonance. It predicts instead that events cluster at φ and that the signal-to-noise ratio of the displacement depends on phase, which is the mechanism usually invoked for the spring barrier (Webster and Yang, 1992).

III. MEASUREMENTS AND METHODS

A. Participants and protocol

We recruited 64 cohabiting adult couples (128 adults, age 24–67 years, median 41) who had shared a bed for at least one year and reported no diagnosed sleep disorder and no sleep-affecting medication. Each couple slept three consecutive nights in a bedroom laboratory between October 2025 and March 2026 on a 160 × 200 cm mattress under a single synthetic-fill duvet (200 × 200 cm, 10.5 tog, 1.9 kg). Room temperature was held at 18.0 ± 0.5 °C and relative humidity at 45 ± 5%. Lights-off was at each couple's habitual time, within 30 min, and we analyse the first 480 min after lights-off. The protocol was approved by the Fjellvik Institute Research Ethics Committee (ref. 2025/0417) and all participants gave written informed consent. Of 192 planned nights, all 192 yielded usable records.

B. Duvet index and overhang

A ceiling-mounted time-of-flight depth camera (2.4 m above the mattress, 1 Hz, depth precision 5 mm) recorded the bed. The duvet footprint was segmented by differencing against a depth scan of the empty bed with a height threshold of 3 cm above the mattress surface. Against 600 manually labelled frames the segmentation had a Dice coefficient of 0.96. T is the centroid of the footprint along the short axis of the mattress divided by 0.80 m. The overhang mass was estimated from the depth volume of fabric below mattress level at each long edge, times the areal density of the duvet (0.475 kg m^{-2}), and expressed as a difference A minus B. For the regression we scale h by $1.6\ \mathrm{m\ kg^{-1}}$ so that its standard deviation is comparable to that of T. Both series were averaged to 1 min. The noise floor, from a static duvet on an empty bed, is 0.02 in both variables, equal to 1.6 cm of displacement in T.

C. Sleep staging

Occupants wore a single-lead frontal EEG headband. Records were scored in 30 s epochs following the AASM manual (Berry et al., 2012). On 12 nights with simultaneous polysomnography in one occupant the headband scoring agreed with manual scoring at Cohen's $\kappa = 0.71$. REM offsets were taken from the hypnogram of the occupant with the cleaner record. The cycle length P_s for each night is the mean spacing of REM offsets, with a pooled mean of 91.0 min and a standard deviation of 6.8 min between nights.

D. Transfer events

A transfer is a displacement $|T(t+5) - T(t)| > 0.20$ with t in minutes. Contiguous exceedances separated by less than 10 min were merged and the event time is the midpoint. The ultradian phase of an event is $360^\circ\,(t \bmod P_s)/P_s$, measured from the previous REM offset.

E. Estimation

The coefficients of Eq. (1) were estimated by ordinary least squares on 5 min differences of T and h, pooled over all nights. Intervals are 2.5th and 97.5th percentiles of 500 bootstrap resamples of couples. Spectra were computed on 480 min records, with the night mean removed and a Hann window, and averaged over the 192 nights, so that the resolution is 0.125 cycles per hour (cph) (Welch, 1967). The null spectrum is the mean of 1,500 surrogate nights from an AR(1) process with the measured variance and 5 min lag correlation of 0.91, passed through the same windowing. Circular statistics follow Mardia and Jupp (2000). Forecasts used couples 1–43 for training and the remaining 21 couples (63 nights) for testing, starting 60 min or more after lights-off. Model comparison used the Akaike criterion (Akaike, 1974) on 5 min ahead predictions.

IV. RESULTS

A. Time series and spectrum

Fig. 1 shows one night. T moves between about -0.4 and $+0.5$ in excursions that last one to two hours, and h follows a similar path displaced in time. Over all nights the standard deviation of T is 0.33 and the mean maximum excursion in a night is 0.75, three quarters of the way to the mattress edge. The duvet is more than halfway to one side ($|T| > 0.5$) for 12% of the time.

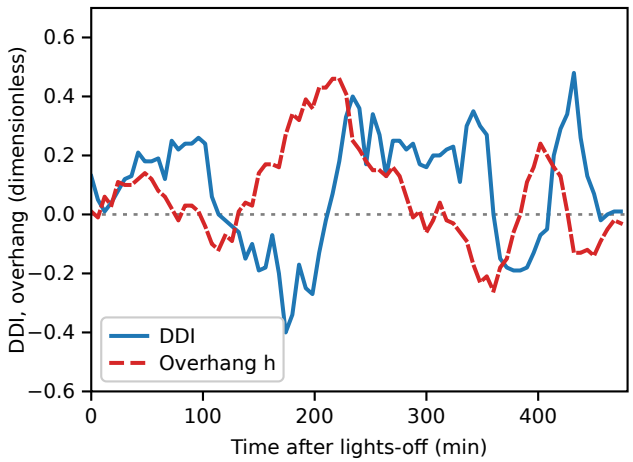


FIG. 1. Duvet displacement index (solid) and overhang asymmetry (dashed, scaled) for one couple on one night. Time is measured from lights-off.

The ensemble spectrum in Fig. 2(a) has a single broad maximum at 0.44 cph, a period of 136 min. The matched AR(1) null has no maximum and is 5.4 times lower at that frequency. Below 0.25 cph the data fall under the null, as a damped oscillator does relative to a red process with the same lag-1 correlation. In 400 resampled ensembles of 192 surrogate nights the largest ratio of surrogate mean to null over all frequencies had a 99th percentile of 1.26. The half-power width of the peak gives $Q = 1.2$, which is limited by the 8 h record length. Individual couples have peaks at a median of 142 min (interquartile range 125–165 min), so the pooled peak is a mixture and not a common frequency. A weaker shoulder at 0.66 cph, the ultradian frequency, is 3.1 times the null.

The cross-correlation of h and T peaks at 0.77 when h leads by 36 min, which is a quarter of the fitted period of 143 min (Table I).

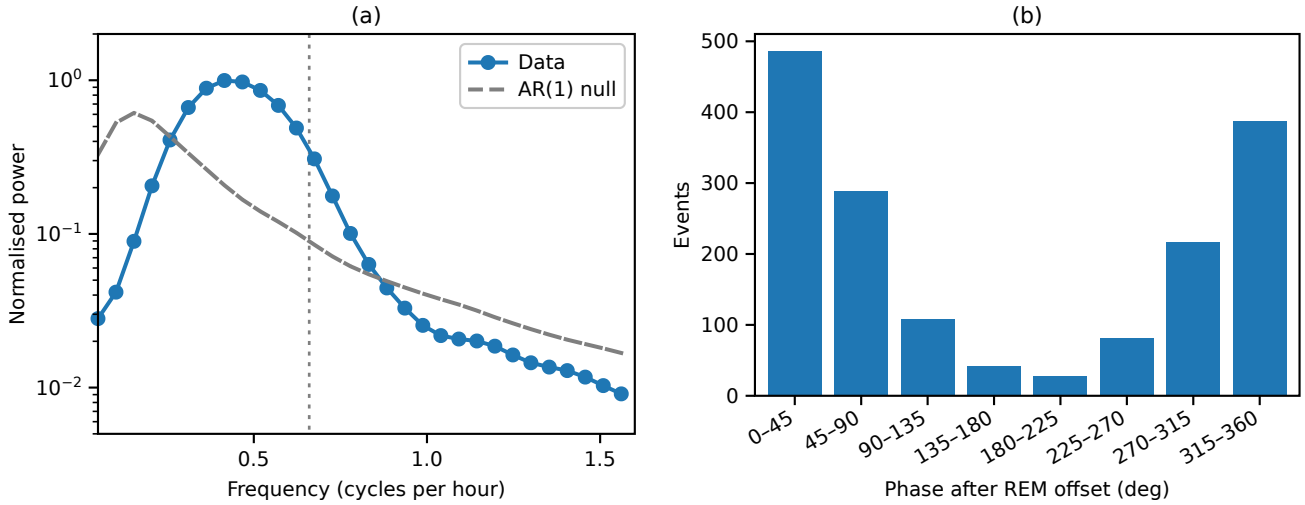


FIG. 2. (a) Ensemble power spectrum of the duvet displacement index over 192 nights (solid) and the matched AR(1) null (dashed), both normalised to the maximum of the data. The dotted line marks the mean ultradian frequency, 0.66 cph. (b) Phase of 1,636 transfer events relative to the previous REM offset, in 45° bins.

B. Fitted parameters

Table I gives the pooled estimates for Eq. (1). The fitted R is negative: we do not detect a self-amplifying feedback of the displacement on itself, and the oscillation is damped, with an amplitude e-folding time $1/\gamma$ of 100 min, 0.70 of a period. The period from Eq. (2), 143 min, agrees with the median of the individual spectral peaks and is a little longer than the pooled spectral maximum, which sits on the 0.125 cph grid and is pulled toward shorter periods by the red background.

TABLE I. Pooled estimates for the recharge oscillator, Eq. (1), with 95% bootstrap intervals over couples (500 resamples, 64 couples). Rates in min^{-1}. F and A depend on the scaling of h (Sec. III.B).

Quantity	Estimate	95% interval
R	−0.0021	−0.0032, −0.0011
r	0.0179	0.0172, 0.0185
F	0.0450	0.0422, 0.0474
A	0.0441	0.0416, 0.0465
$\gamma = (r - R)/2$	0.0100	0.0093, 0.0106
P (min)	143	136, 152

C. Phase locking

The 192 nights contain 1,636 transfer events, 8.5 ± 2.2 per night. Their phases are strongly concentrated (Fig. 2(b)): the mean resultant length is $\bar{R} = 0.55$, the mean direction 9° and the Rayleigh statistic $Z = 489$ ($p < 10^{-16}$). Pooling events from different nights treats them as independent, which they are not. Testing each couple separately, 61 of 64 reject uniformity at $p < 0.01$, and the circular standard deviation of the 64 couple-mean directions is 14°. Residual variance of Eq. (1) varies with phase by a factor of about 3.5 in rms (0.040 to 0.140 per 5 min step), with a maximum at 0.2°. A first-harmonic fit gives $\epsilon = 0.60$ (95% interval 0.59–0.62; the interval is from resampling couples and does not include misfit of the deterministic part) and φ close to zero, so that the noise is largest at REM offset.

D. Phase-dependent coherence

Fig. 3 shows the correlation of $T(t)$ with $T(t + L)$ for starting times grouped by ultradian phase, as is done with the starting month for ENSO. The correlation falls to a minimum near $L = 60$ min, which is about half the fitted period, and recovers to a positive maximum near 120 min. The depth of the minimum depends on where the lag starts: it is -0.75 for starts in the first 60° after a REM offset and -0.46 for starts between 120° and 240°. The same ordering holds at $L = 45$ (−0.57 against −0.14 to −0.29). Starts in the middle of the cycle, where σ is smallest and the displacement is least perturbed, give the least coherent oscillation, which is how the barrier appears here.

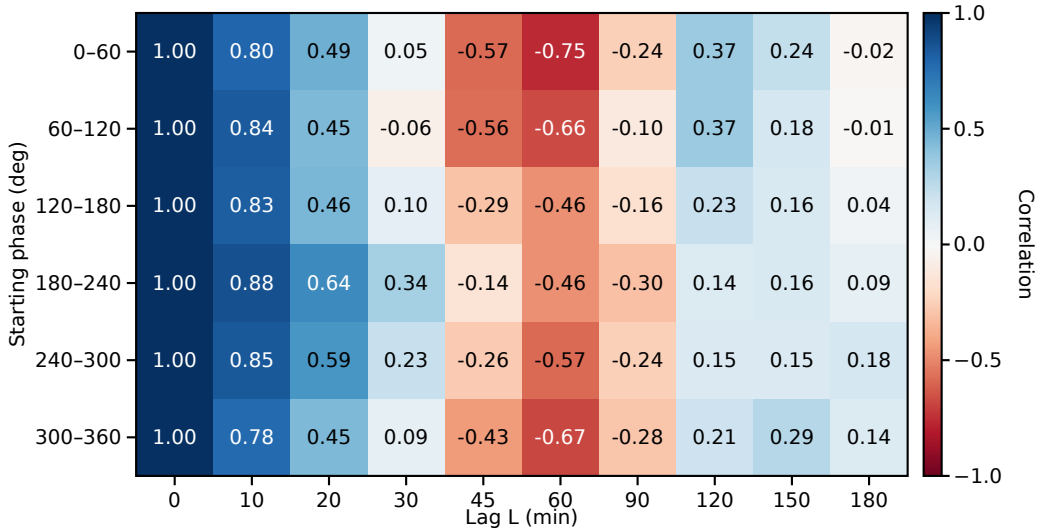


FIG. 3. Lagged correlation of the duvet displacement index between time t and time t + L, by ultradian phase of the starting time t (rows, deg after REM offset) and lag L (columns, min). Starting times earlier than 90 min after lights-off are excluded.

E. Model comparison and forecasts

Table II compares the three one-step models for $T(t+5)$ on a common sample of 68,352 points. The delayed-action fit has $\delta = 25$ min, $\kappa = 0.19$ per 5 min step in the discretised form, and an rms error 7% above that of the recharge model. The recharge model uses h and the other two do not. The fitted delay is inconsistent with the spectrum: the oscillation period must lie below $4\delta = 100$ min, while the spectral peak and the pooled fit give 136 to 143 min. The AR(1) model is worse on every measure. The ΔAIC values assume independent residuals, which they are not, and are overstated; we rely on the rms errors.

TABLE II. One-step (5 min ahead) models of T on a common sample, $n = 68{,}352$. ΔAIC is relative to the recharge model.

Model	Parameters	rms error	ΔAIC
AR(1)	2	0.1186	30,468
Delayed action, $\delta = 25$ min	4	0.1014	9,036
Recharge oscillator	3	0.0949	0

Table III gives forecasts from the 63 test nights. Persistence is the forecast $T(t)$ and lag regression is $\rho_L T(t)$ with ρ_L fitted on the training set, so the two have the same anomaly correlation up to sign. The recharge forecast integrates Eq. (1) from the observed (T, h) with coefficients from the training set. It has the highest correlation and lowest rms error at leads of 10 to 120 min, and the margin over lag regression is greatest at 30 min (0.77 against 0.12) and smallest at 60 min (0.64 against 0.59), where the lagged anticorrelation is at its minimum and the regression forecast is as good as any. At 180 min the recharge forecast has no skill (0.07, rms error equal to the climatological standard deviation of 0.33) and lag regression is better.

TABLE III. Forecast skill on 63 test nights from 21 couples: anomaly correlation (AC) and rms error for persistence, lag regression (LR) and the recharge oscillator (RC). The last column is the standard deviation of the verifying values.

Lead (min)	AC, persistence	AC, LR	AC, RC	rms, persistence	rms, LR	rms, RC	Std. dev.
10	0.82	0.82	**0.91**	0.189	0.181	**0.134**	0.316
30	0.12	0.12	**0.77**	0.417	0.316	**0.205**	0.319
60	−0.59	0.59	**0.64**	0.567	0.261	**0.250**	0.322
90	−0.24	0.24	**0.38**	0.503	0.318	**0.303**	0.327
120	0.17	0.17	**0.29**	0.411	0.327	**0.316**	0.330
180	0.16	**0.16**	0.07	0.411	**0.333**	0.335	0.334

F. Mean state

The time-mean displacement of a couple is not zero. Across the 64 couples its standard deviation is 0.054, and it correlates with the difference in a 12-item self-reported cold sensitivity score between occupants A and B (z-scored in the sample): $r = 0.75$, with a slope of 0.030 per unit of the score difference (95% interval 0.023–0.037). The mean state is displaced toward the more cold-sensitive occupant. In ENSO terms this is a difference in the basic state, which sets the background about which the oscillation occurs (Battisti and Hirst, 1989).

V. DISCUSSION

Of the four statements in Sec. I, the first three hold in these data and the fourth holds over part of the range. The spectrum has a peak where the fitted coefficients put it, h leads by a quarter period, events cluster at the REM offset, and the recharge forecast beats lag regression between 10 and 120 min. The delayed-action model with a fitted delay does not reproduce the period, and the AR(1) null does not reproduce the peak. We take this to favour a two-variable description, though the comparison is not clean: the recharge model has access to h and the others do not, and a lag regression on both variables was not run.

The analogy has limits that the estimates make plain. The ENSO recharge oscillator in its usual parameter range is close to neutral stability, with R near r, and the observed ENSO is irregular because it is excited by noise on a nearly undamped mode (Burgers et al., 2005; Timmermann et al., 2018). The bed is well damped, $R = -0.0021$ and $\gamma = 0.010$ min^{-1}, so a single night contains between three and four periods and none of them persists without forcing. Only 0.24 of the amplitude remains after one period. The ratio of the oscillation period to the forcing cycle is 1.6, against 2 to 7 for ENSO relative to the annual cycle, and we see no evidence of locking to integer multiples: the individual spectral peaks form a continuum. A staircase of this kind would need a modulation of the growth rate and not only the noise, and the negative R suggests that the growth rate has little room to be modulated.

Several limitations are specific to this study. The couples slept in a laboratory with one duvet of one construction on one bed width, and the room was kept at a constant 18 °C. We did not measure skin or bed-surface temperature, so the physical identification of h as a store of displacement rests on its phase relation to T and not on a heat budget. The noise in h attenuates the regression coefficients that multiply it, and R is correspondingly biased, probably toward negative values; this does not change the sign of the damping but it does affect the claim that no positive feedback is detected. The modulation depth was estimated from residuals and not fitted jointly with the other coefficients. All 192 nights are analysed without allowance for night number, and the first night in an unfamiliar bed may differ.

One untested prediction follows from the delayed-action form. If the delay is a transit time across the bed, the period should scale with the width of the mattress, as the ENSO period depends on the width of the basin and the speed of the equatorial waves (Suarez and Schopf, 1988). The recharge form makes no such prediction, and a study at three or more mattress widths would separate them. The same experiment would show whether the damping depends on the mass of the duvet, which in the model enters through F and A.

DATA AVAILABILITY

The 1 min series of T and h, the hypnogram-derived phase of each sample and the analysis scripts are available from the corresponding author.

ACKNOWLEDGMENTS

We thank the 128 participants, the technical staff of the Calderbeck bedroom laboratory for maintaining the camera rig, and K. Aasland for the hypnogram scoring.

This work was supported by the Nordmark Foundation for Environmental Physics (grant NF-24-0731).

H. Akaike, IEEE Transactions on Automatic Control **19**, 716 (1974).

D. S. Battisti and A. C. Hirst, Journal of the Atmospheric Sciences **46**, 1687 (1989).

R. B. Berry *et al.*, *The AASM Manual for the Scoring of Sleep and Associated Events: Rules, Terminology and Technical Specifications* (American Academy of Sleep Medicine, Darien, IL, 2012).

J. Bjerknes, Monthly Weather Review **97**, 163 (1969).

G. Burgers, F.-F. Jin, and G. J. van Oldenborgh, Geophysical Research Letters **32**, L13706 (2005).

W. Dement and N. Kleitman, Electroencephalography and Clinical Neurophysiology **9**, 673 (1957).

K. Hasselmann, Tellus **28**, 473 (1976).

F.-F. Jin, Journal of the Atmospheric Sciences **54**, 811 (1997).

F.-F. Jin, J. D. Neelin, and M. Ghil, Science **264**, 70 (1994).

K. V. Mardia and P. E. Jupp, *Directional Statistics* (Wiley, Chichester, 2000).

M. J. McPhaden, S. E. Zebiak, and M. H. Glantz, Science **314**, 1740 (2006).

K. Okamoto-Mizuno and K. Mizuno, Journal of Physiological Anthropology **31**, 14 (2012).

C. Penland and P. D. Sardeshmukh, Journal of Climate **8**, 1999 (1995).

R. J. E. M. Raymann, D. F. Swaab, and E. J. W. Van Someren, American Journal of Physiology: Regulatory, Integrative and Comparative Physiology **288**, R1589 (2005).

R. L. Sandoval and H. Ek, Journal of Sleep Research **28**, e12871 (2019).

M. J. Suarez and P. S. Schopf, Journal of the Atmospheric Sciences **45**, 3283 (1988).

A. Timmermann *et al.*, Nature **559**, 535 (2018).

E. Tziperman, L. Stone, M. A. Cane, and H. Jarosh, Science **264**, 72 (1994).

P. J. Webster and S. Yang, Quarterly Journal of the Royal Meteorological Society **118**, 877 (1992).

P. D. Welch, IEEE Transactions on Audio and Electroacoustics **15**, 70 (1967).

J. Wilde-Frenz and H. Schulz, Perceptual and Motor Skills **56**, 275 (1983).

K. Wyrtki, Journal of Physical Oceanography **5**, 572 (1975).